ISSN 1028-334X, Doklady Earth Sciences, 2006, Vol. 411, No. 8, pp. 1257–1262. © Pleiades Publishing, Inc., 2006.
Original Russian Text © Yu.Yu. Golubeva, V.A. Pervov, V.A. Kononova, 2006, published in Doklady Akademii Nauk, 2006, Vol. 410, No. 6, pp. 789–794.

GEOCHEMISTRY

Petrogenesis of Autoliths from Kimberlitic Breccias in the V. Grib Pipe (Arkhangelsk District)

Yu. Yu. Golubeva, V. A. Pervov, and V. A. Kononova

Presented by Academician I.D. Ryabchikov June 29, 2006

Received July 4, 2006

DOI: 10.1134/S1028334X06080228

Kimberlitic diatremes are primarily composed of autolithic kimberlitic breccia. The name of this variety of kimberlitic rocks is related to the specific distribution of autoliths in the matrix. According to [1–3], autoliths are prominent fragments of kimberlitic breccia. The autoliths are also known as kimberlite-type inclusions in kimberlite, inclusions of kimberlites of earlier generations, fragments of magmatic kimberlite, pellets, and lapillies. The shape of these rocks can be both rounded (the shell smoothes out the irregular surface of the core) and irregular (with inlets and projections). The content of autoliths in the breccia is 10–20% (in some places, 50% or more), while their dimension varies from 0.*n* mm to 10–15 cm. The autoliths can occur as core-bearing and core-free varieties. In the first case, the core can be composed of xenoliths of enclosing and mantle rocks or rimmed crystals of minerals. Distinct cores are not constant attributes of large autoliths. The maximal dimension is typical of autoliths with xenolith as the core. The autoliths can be surrounded by porphyric or aphyric rims. Some autoliths demonstrate a fluidal (concentric-zonal) texture. The concentrations of TiO_2, Al_2O_3, K_2O, P_2O_5, and FeO in these rocks are reflected in their mineral composition. They are commonly darker than the enclosing breccia due to high contents of fine grains of ore minerals and occasional mica flakes [2–4]. In the autolithic kimberlitic breccias of kimberlite pipes, the autoliths are similar to plutonic rocks in composition and texture [2–5]. According to [2, 3], both fluidal and massive varieties of the autolith show similar trends of changes in the chemical composition.

In order to check regularities defined in previous works, we investigated the geochemistry of autolithic kimberlitic breccias and autoliths from kimberlites of the V. Grib Pipe (Zimnii Bereg diamondiferous province, Verkhotinskoe field). The V. Grib Pipe stands out among other kimberlites of the Arkhangelsk district in the diamond potential, geology, and mineralogy scrutinized in several publications [4, 6, and others]. At present, this kimberlite pipe has been explored to a depth of more than 900 m. The pipe includes rocks of the crater (110 m) and vent facies mainly represented by autolithic kimberlitic breccias. We studied the autolithic kimberlitic breccias and autoliths recovered at the depth interval of 590–690 m from borehole 106 (Fig. 1). The studied autoliths are characterized by rounded and irregular shapes, and their dimension ranges from 3 × 4 to 5 × 6 cm. Except sample 106/628A, which includes a core of acid metamorphic rock, all other autolith samples are represented by the core-free version with textures ranging from the megaphyric to the microphyric variety. Autoliths in samples 106/627A and 106/628A include carbonate–serpentine–diopside globules. When preparing breccia samples for high-precision analysis, we paid special attention to the removal of xenogenic material, the content of which did not exceed 5% at the studied depths. We carried out the ICP-MS analysis of REEs at the Vernadsky Institute of Geochemistry and Analytical Chemistry, Moscow (D.Z. Zhuravlev, analyst), and the Sr–Nd isotope analysis at the Institute of Precambrian Geology and Geochronology, St. Petersburg. The results obtained are presented in Tables 1–3 and Figs. 2–4. The results of the comparison of the petrochemistry of autoliths and the whole-rock composition of breccias (Table 1) are consistent with the data presented by other researchers [2–5]. Although the compositions of the autolithic kimberlitic breccia (whole-rock) and autolith are slightly different, they retain features typical of Yakutian kimberlites [3, 5]. For example, relative to the autolithic kimberlitic breccias, the autoliths are enriched in Ti, Al, Fe, K, and P. Only the carbonate component shows some differences from the trends previously recorded for the Yakutian kimberlites. For example, relative to kimberlites in other regions, autoliths from kimberlites of the V. Grib Pipe are

Institute of Geology of Ore Deposits, Petrography, Mineralogy, and Geochemistry, Russian Academy of Sciences, Staromonetnyi per. 35, Moscow, 119017 Russia;
e-mail: golubeva@igem.ru

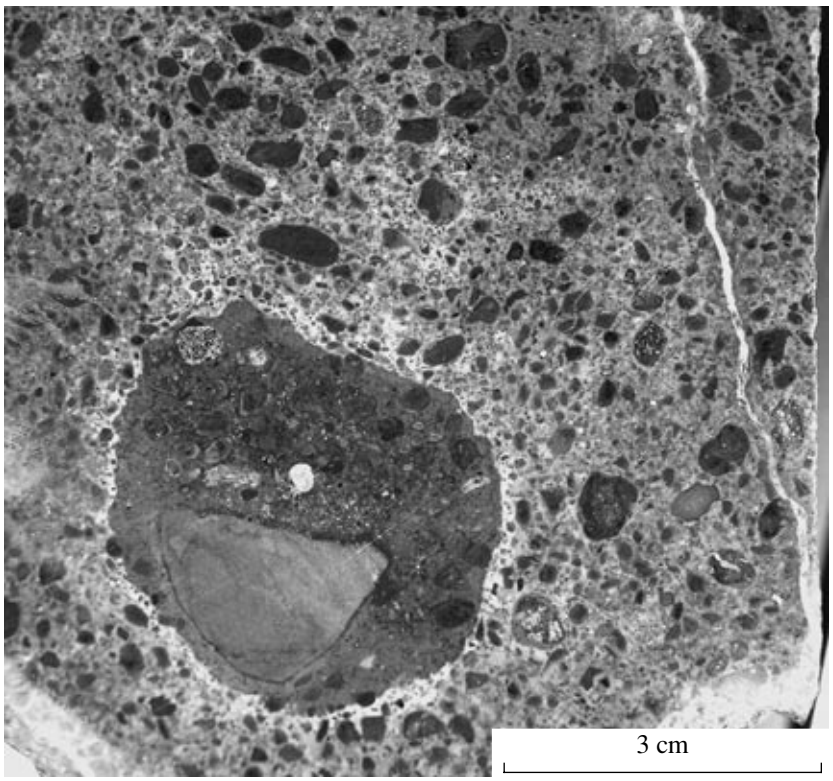

Fig. 1. Autolithic kimberlitic breccia (sample 106/606) from the V. Grib Pipe and megaphyric autolith with core composed of host rock xenolith.

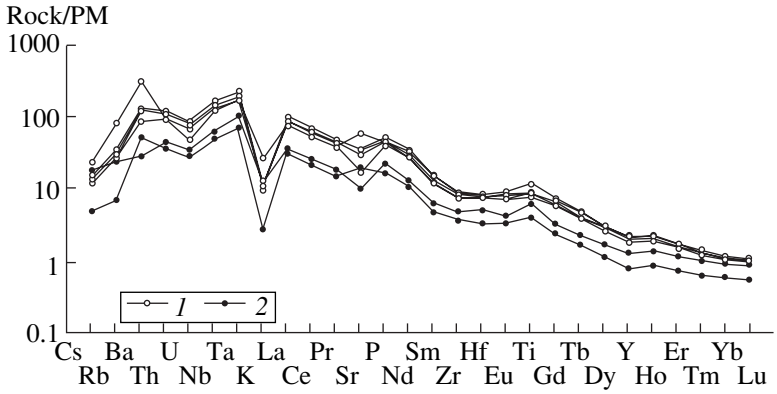

Fig. 2. PM-normalized [9] REE distribution in autolithic kimberlitic breccias and autoliths from the V. Grib Pipe. Legend for Figs. 2–4: (*1*) Autolith; (*2*) autolithic kimberlitic breccia.

enriched in CO_2 and CaO. According to Ilupin [3], carbonate from the Yakutian kimberlites could be redistributed at the postmagmatic stage. We failed to detect any regular changes in concentrations of Si, Mg, and water at the autolithic kimberlitic breccia–autolith transition zone (Table 1).

It is evident from the results (Table 2; Figs. 2, 3) that, relative to the bulk composition of kimberlitic breccias, the autoliths are much more enriched in some elements, such as Cr, Sc, Hf, Ta, Th, and REE, which are stable during secondary alterations. The REE distribution plot (Fig. 2) also shows that, relative to the kimberlites, the autoliths are enriched in all incoherent elements. Among all autolith samples, sample 106/627A is distinguished by high concentrations of Ba, Sr, and Rb, probably owing to the high contents of carbonate in this sample (carbonate–serpentine–diopside globules). The autoliths are enriched in the REEs, particularly, LREEs (2.1–3.1 times, on average), while the HREE concentrations are 1.2–2.2 times higher. Therefore, the

Table 1. Compositions of autolithic kimberlitic breccias (AKB) and autoliths in borehole 106, V. Grib Pipe (wt %)

Component	AKB		Autoliths from kimberlites in borehole 106				
	106/606	106/590	106/612A	106/627A	106/628A	106/630A	106/690A
SiO_2	40.81	36.51	33.78	33.52	32.88	33.81	35.07
TiO_2	1.39	0.97	1.90	1.65	2.33	1.96	1.95
Al_2O_3	1.72	1.30	1.84	1.96	2.18	2.58	1.69
Fe_2O_3	4.16	6.02	4.05	4.21	4.96	4.54	4.11
FeO	3.06	1.93	3.75	3.25	3.25	3.67	3.82
MgO	31.83	36.35	31.45	29.46	30.49	29.70	33.11
MnO	0.15	0.12	0.14	0.15	0.15	0.15	0.16
CaO	3.70	3.25	6.84	8.37	7.14	6.63	4.45
Na_2O	0.38	0.10	0.13	0.19	0.16	0.15	0.15
K_2O	0.31	0.07	0.27	0.68	0.24	0.33	0.27
P_2O_5	0.22	0.16	0.43	0.41	0.47	0.42	0.37
L.O.I.	12.45	11.96	15.03	15.61	15.59	15.04	12.82
Total	100.18	98.74	99.61	99.46	99.85	98.98	97.97
CO_2	0.54	0.56	3.91	4.94	4.14	3.77	2.45
H_2O^+	11.91	10.97	11.12	10.67	11.45	11.27	10.37
C.I.	1.32	1.04	1.12	1.16	1.14	1.20	1.10
mg#	0.82	0.82	0.80	0.80	0.79	0.78	0.81

Note: (C.I.) Contamination index $(SiO_2 + Al_2O_3 + Na_2O)/(2K_2O + MgO)$ [7]; Mg index, mg# = $MgO/(MgO + FeO_t)$.

La/Yb ratio is higher in the autoliths (108–129) than in the autolithic kimberlitic breccias (57–76).

The concentrations of rare elements and REEs are virtually similar in the autoliths (Figs. 2, 3). In the autolithic kimberlitic breccias, these elements demonstrate a significant scatter of values. This is seen in Fig. 3, which also includes our data on the autolithic kimberlitic breccias from other boreholes drilled in the V. Grib Pipe area. In addition, this diagram shows a direct correlation between the autoliths and kimberlites with respect to the Ti_2O versus HREE, Zr, Ce, and Y relationship.

However, the autolithic kimberlitic breccias and autoliths from the V. Grib Pipe show different Sr–Nd isotope characteristics (Table 3, Fig. 4). In Fig. 4, data points of primary isotope ratios fall into the Bulk Silicate Earth (BSE) field. Moreover, the autolithic kimberlitic breccias are more enriched than the autoliths relative to the depleted mantle. The data points of the autoliths make up a relatively compact cluster, except for some variations in the ε_{Sr} field. The autolithic kimberlitic breccias have a more enriched isotopic composition, probably owing to contamination with the lower crustal material.

Thus, kimberlitic breccias and autoliths from the V. Grib Pipe clearly demonstrate compositional differences. This fact is essential for understanding the petrogenesis of autoliths of this kimberlite pipe. Identification of such discrepancies can ultimately be used in the generalized model of diamondiferous kimberlite pipes.

According to the popular magmatic model of the formation of autolithic rocks presented by Mitchell [11], the injection of melts is accompanied by rapid fractionation of volatiles from the melts and the transportation of a portion of magma in the fluid system. Autoliths can form if the magma ascent rate is high. Fractionation of volatile phases and mixing of the magma trigger its fragmentation. These processes foster the formation of magma drops and exhumation of the partially recrystallized magma. We believe that the V. Grib Pipe formed as a result of exhumation of the kimberlitic magma, its partial recrystallization, and formation of autoliths enriched in rare elements. This scenario is valid not only for kimberlites, but also for other alkaline-ultrabasic rocks. According to the formation model of fluidal autoliths in kamafugite diatremes presented in [12], the autoliths are formed as a result of the rotation of magma drops in the fluidized system.

The model proposed by Krivoshlyk [5] and supported by other researchers [3, 4, 13] considers the behavior of kimberlitic magma before its eruption. According to this model, the eruption of magma is preceded by fractionation of the H_2O–CO_2 fluid. The con-

Table 2. Rare elements (ppm) in autolithic kimberlitic breccias (AKB) and autoliths in borehole 106, V. Grib Pipe (ICP-MS data)

Element	AKB		Autoliths from kimberlites in borehole 106				
	106/606	106/590	106/612A	106/627A	106/628A	106/630A	106/690A
Be	1.00	1.456	1.42	3.22	1.95	2.16	1.92
Sc	4.5	7.4	9.6	8.2	11.3	10.0	8.7
V	91	75	138	170	165	142	130
Cr	1256	907	1635	1673	2233	1889	1850
Mn	800	785	867	929	959	944	1038
Co	77	88	74	71	68	76	76
Ni	1679	1346	1391	1361	1420	1447	1562
Cu	99	133	568	460	760	458	83
Zn	98	56	65	57	70	67	59
Ga	3.2	3.0	4.4	4.8	5.6	5.1	4.2
Rb	15.2	4.2	16.3	49.0	16.4	21.8	17.8
Sr	215	407	708	1201	709	617	345
Y	5.8	3.6	9.3	8.3	9.8	9.8	8.3
Zr	54	40	87	87	94	91	80
Nb	43	34	93	86	110	99	85
Mo	0.48	2.68	0.53	1.19	1.35	1.32	1.32
Cs	0.38	0.11	0.31	0.50	0.26	0.30	0.31
Ba	196	351	848	2072	873	826	585
La	24.8	21.6	57.6	52.6	65.9	62.5	52.7
Ce	45.2	38.3	100.7	93.5	116.3	110.6	93.4
Pr	4.82	4.01	11.09	10.05	12.54	12.00	10.08
Nd	16.77	13.93	39.52	36.19	44.79	42.44	35.38
Sm	2.63	1.96	5.62	5.17	6.25	6.10	5.05
Eu	0.679	0.547	1.366	1.118	1.459	1.319	1.131
Gd	1.862	1.367	3.685	3.370	4.107	3.925	3.309
Tb	0.240	0.177	0.442	0.413	0.501	0.480	0.400
Dy	1.214	0.811	2.072	1.887	2.163	2.166	1.843
Ho	0.215	0.141	0.335	0.310	0.346	0.358	0.310
Er	0.541	0.339	0.772	0.727	0.785	0.815	0.710
Tm	0.073	0.046	0.095	0.089	0.095	0.105	0.087
Yb	0.437	0.283	0.522	0.487	0.511	0.547	0.466
Lu	0.064	0.039	0.080	0.079	0.076	0.078	0.069
Hf	1.51	0.99	2.17	2.27	2.40	2.30	2.15
Ta	4.03	2.70	6.93	6.71	8.47	7.44	6.63
Th	3.76	3.07	8.54	7.84	9.48	9.22	7.79
U	0.73	0.58	1.53	1.38	1.69	1.57	0.99

sequent liquid immiscibility of the kimberlitic magma is responsible for the generation of two secondary melts. The ultrabasic silicate component produces the autoliths, while the carbonatitic component produces the breccia cement. This model has been experimentally confirmed for the reaction between spinel peridotite and H_2O–CO_2 fluid [13]. The experiments have shown that Si, Al, and Ti correlate with the aqueous gas phase, while Mg and Ca correlate with CO_2. In the Yakutian kimberlites, CO_2 is preferentially concentrated in the matrix, while H_2O is concentrated in the autoliths. This reliably established fact supports the model mentioned above [1–3, 5, 13]. However, kimberlites from the V. Grib Pipe demonstrate an inverse cor-

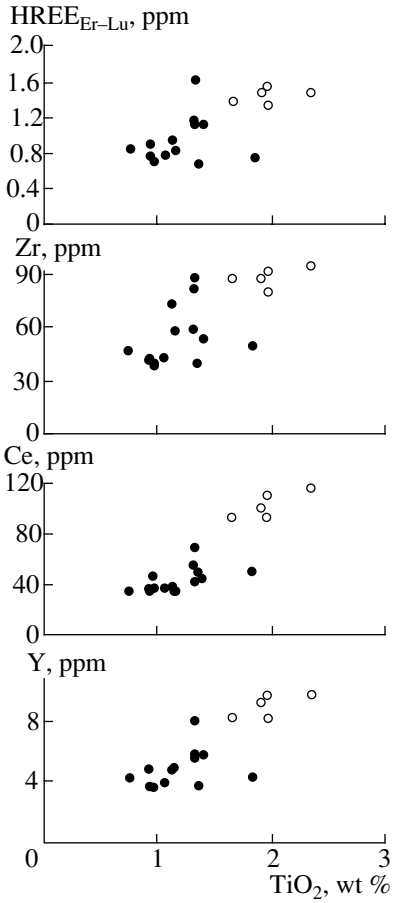

Fig. 3. TiO_2 vs. HREE, Zr, Ce, and Y relationship in autolithic kimberlitic breccias and autoliths from the V. Grib Pipe.

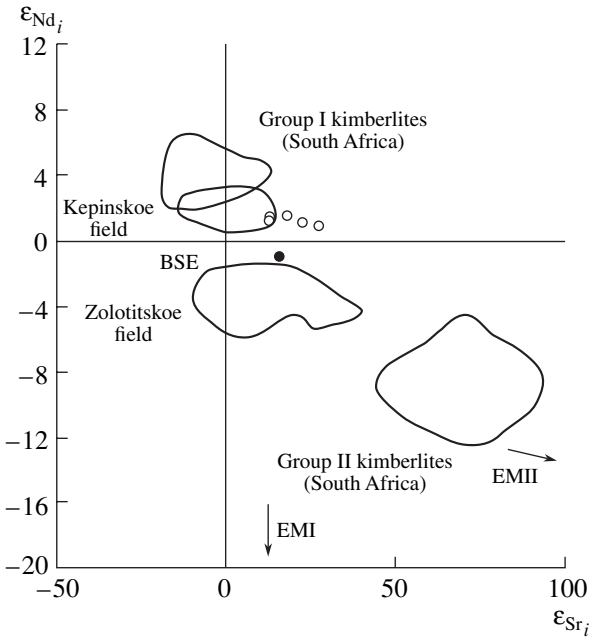

Fig. 4. ε_{Nd}–ε_{Sr} diagram for autolithic kimberlitic breccias and autoliths from the V. Grib Pipe (fields are based on [10]).

relation. Therefore, we cannot consider the autoliths as immiscibility products.

In conclusion, we should note that further investigation of all varieties of autoliths is essential for more complete understanding of their petrogenesis. Their formation is evidently related to the interaction between fluids and magmas. Petrographic and geochemical patterns of autolithic kimberlitic breccias in kimberlite pipes depend on the behavior of fluids before and during magma eruption. For example, the model proposed by Mitchell [11] is most suitable for explaining the formation of autoliths in the V. Grib Pipe. At the same time, one should take into account the fact that some autoliths in the breccias can be related to the entrapment of fragments from older, cooled portions of kimberlite. In other words, kimberlite pipes can be formed in several phases owing to the recurrence of eruptions, crushing of older rocks, and cementa-

Table 3. Nd–Sr isotope data on autoliths and autolithic kimberlitic breccias from the V. Grib Pipe

Sample no.	Rb, ppm	Sr, ppm	$^{87}Rb/^{86}Sr$	$^{87}Sr/^{86}Sr$	$(^{87}Sr/^{86}Sr)_t$	ε_{Sr_i}
106/606	15.48	211.6	0.2116	0.706251 ± 14	0.705127	+15
106/612A	16.86	717.0	0.0680	0.705969 ± 10	0.705608	+22
106/627A	50.70	1259.0	0.1165	0.706563 ± 19	0.705944	+27
106/628A	16.15	690.7	0.0676	0.705656 ± 7	0.705297	+18
106/630A	22.27	631.9	0.1019	0.705475 ± 12	0.704934	+12
106/690A	16.02	339.7	0.1364	0.705640 ± 17	0.704915	+12
Sample no.	Sm, ppm	Nd, ppm	$^{147}Sm/^{144}Nd$	$^{143}Nd/^{144}Nd$	$(^{143}Nd/^{144}Nd)_t$	ε_{Nd_i}
106/606	2.39	16.06	0.0898	0.512328 ± 11	0.512109	–1.0
106/612A	5.16	36.77	0.0848	0.512422 ± 8	0.512215	+1.1
106/627A	4.56	32.36	0.0851	0.512413 ± 10	0.512205	+0.9
106/628A	5.61	40.20	0.0843	0.512441 ± 9	0.512235	+1.5
106/630A	5.59	39.81	0.0848	0.512440 ± 6	0.512233	+1.5
106/690A	4.63	33.07	0.0846	0.512426 ± 10	0.512219	+1.2

Note: Primary isotope ratios, ε_{Nd_i}, and ε_{Sr_i} values were calculated at t = 373 Ma [8] with consideration of UR isotope ratios ($^{87}Rb/^{86}Sr$ = 0.825 and $^{87}Sr/^{86}Sr$ = 0.7045) and CHUR values ($^{147}Sm/^{144}Nd$ = 0.1967 and $^{143}Nd/^{144}Nd$ = 0.512638).

tion of breccias by new portions of magma. This mechanism can be responsible for the clastic appearance of some autoliths.

ACKNOWLEDGMENTS

This work was supported by the Russian Foundation for Basic Research (project no. 06-05-64017) and the Foundation of the President of the Russian Federation for the Support of Leading Scientific Schools and Young Scientists (project nos. MK-5814.2006.5 and 02.445.11.7255, respectively).

REFERENCES

1. V. P. Kornilova, K. N. Nikishov, V. V. Koval'skii, and G. V. Zol'nikov, in *Atlas of Structures and Textures of Kimberlitic Rocks* (Nuaka, Moscow, 1983) [in Russian].
2. I. P. Ilupin, A. A. Lebedev-Zinov'ev, and A. I. Kryuchkov, in *Specific Features of the Within-Plate Basic Magmatism* (Moscow, 1980), pp. 173–184 [in Russian].
3. I. P. Ilupin, Otechest. Geol., No. 3, 63 (2000).
4. A. A. Burmistrov, K. V. Garanin, V. I. Starostin, and L. S. Yuzhakov, in *Geology of Diamonds: Present and Past (Essays of Geologists Devoted to the 50th Anniversary of Mirnyi and Russia's Diamond Development Industry)* (Voronezh State Univ., Voronezh, 2005), pp. 762–772 [in Russian].
5. I. N. Krivoshlyk, Dokl. Akad. Nauk **252**, 190 (1980).
6. O. A. Bogatikov, V. K. Garanin, V. A. Kononova, et al., *The Arkhangelsk Diamondiferous Province: Geology, Petrography, Geochemistry, and Mineralogy* (MGU, Moscow, 1999) [in Russian].
7. W. R. Taylor, L. A. Tompkins, and S. E. Haggerty, Geochim. Cosmochim. Acta **58**, 4017 (1994).
8. V. A. Larchenko, V. P. Stepanov, G. V. Minchenko, and V. A. Pervov, in *Geology of Diamonds: Present and Past (Essays of Geologists Devoted to the 50th Anniversary of Mirnyi and Russia's Diamond Development Industry)* (Voronezh State Univ., Voronezh, 2005), pp. 322–347 [in Russian].
9. W. F. McDonough and S.-S. Sun, Chem. Geol. **120**, 223 (1995).
10. O. A. Bogatikov, V. A. Kononova, V. A. Pervov, and D. Z. Zhuravlev, Petrology, No. 3, 191 (2001) [Petrologiya, No. 3, 227 (2001)].
11. R. H. Mitchell, *Mineralogy, Geochemistry, and Petrology* (Plenum Press, New York, 1986).
12. T. C. Junqueira-Brod, J. A. Brod, R. N. Thompson, and S. A. Gibson, Rev. Brasil. Geoclênc. **29**, 437 (1999).
13. V. I. Vaganov, *Diamond Deposits of Russia and the World (Principles of Forecasting)* (ZAO Geoinformmark, Moscow, 2000) [in Russian].